

# Osteoarthritis and Cartilage



## Deficiency of hyaluronan synthase 1 (*Has1*) results in chronic joint inflammation and widespread intra-articular fibrosis in a murine model of knee joint cartilage damage



D.D. Chan †, W.F. Xiao ‡, J. Li †, C.A. de la Motte §, J.D. Sandy || ¶, A. Plaas † †\*

† Division of Rheumatology, Department of Internal Medicine, Rush University Medical Center, Chicago, IL, USA

‡ Department of Orthopedics, Xiangya Hospital, Central South University, Changsha, Hunan, China

§ Department of Pathobiology, Lerner Research Institute, Cleveland Clinic, Cleveland, OH, USA

|| Department of Biochemistry, Rush University Medical Center, Chicago, IL, USA

¶ Department of Orthopedic Surgery, Rush University Medical Center, Chicago, IL, USA

### ARTICLE INFO

#### Article history:

Received 5 December 2014

Received in revised form

25 June 2015

Accepted 28 June 2015

#### Keywords:

Cartilage  
Injury  
Synovium  
Inflammation  
Fibrotic scar  
Hyaluronan synthases

### SUMMARY

**Objective:** Articular cartilage defects commonly result from traumatic injury and predispose to degenerative joint diseases. To test the hypothesis that aberrant healing responses and chronic inflammation lead to osteoarthritis (OA), we examined spatiotemporal changes in joint tissues after cartilage injury in murine knees. Since intra-articular injection of hyaluronan (HA) can attenuate injury-induced osteoarthritis in wild-type (WT) mice, we investigated a role for HA in the response to cartilage injury in mice lacking HA synthase 1 (*Has1*<sup>-/-</sup>).

**Design:** Femoral groove cartilage of WT and *Has1*<sup>-/-</sup> mice was debrided to generate a non-bleeding wound. Macroscopic imaging, histology, and gene expression were used to evaluate naïve, sham-operated, and injured joints.

**Results:** Acute responses (1–2 weeks) in injured joints from WT mice included synovial hyperplasia with HA deposition and joint-wide increases in expression of genes associated with inflammation, fibrosis, and extracellular matrix (ECM) production. By 4 weeks, some resurfacing of damaged cartilage occurred, and early cell responses were normalized. Cartilage damage in *Has1*<sup>-/-</sup> mice also induced early responses; however, at 4 weeks, inflammation and fibrosis genes remained elevated with widespread cartilage degeneration and fibrotic scarring in the synovium and joint capsule.

**Conclusions:** We conclude that the ineffective repair of injured cartilage in *Has1*<sup>-/-</sup> joints can be at least partly explained by the markedly enhanced expression of particular genes in pathways linked to ECM turnover, IL-17/IL-6 cytokine signaling, and apoptosis. Notably, *Has1* ablation does not alter gross HA content in the ECM, suggesting that HAS1 has a unique function in the metabolism of inflammatory HA matrices.

© 2015 Osteoarthritis Research Society International. Published by Elsevier Ltd. All rights reserved.

### Introduction

Traumatic injuries to articular cartilage of the knee can result from excessive surface contact stresses after blunt impact or torsion, which occur frequently during sports and military training<sup>1</sup>. Resulting patellar dislocation<sup>2</sup>, joint incongruity, and instability can

predispose to osteoarthritis (OA)<sup>3</sup>. Responses to cartilage injury share many features of wound healing, such as innate inflammation<sup>4</sup> and activation of multipotent progenitor cells in the synovium or the articular surface<sup>5</sup>. However, in many cases, the repair response leads to fibrotic remodeling and scarring of the joint lining tissues, subchondral bone sclerosis, and chondrocyte or osteophyte development at the articular margins.

Whereas chronic inflammation is widely recognized as a driving factor in OA, the concept of a pathogenic role for fibrotic scarring is less well-studied<sup>6</sup>. Evidence for focal scarring has been reported for synovial tissue and cartilages from both animal model and human OA<sup>7</sup>, each of which exhibit activation of multiple genes associated with collagen production and deposition (*CRLF1*, *PLOD2*, *LOX*,

\* Address correspondence and reprint requests to: A. Plaas, 1653 West Congress Parkway, Jelke Building, Suite 1413, Chicago, IL 60612, USA. Tel: 1-312-942-7194; Fax: 1-312-563-2267.

E-mail addresses: [deva\\_chan@rush.edu](mailto:deva_chan@rush.edu) (D.D. Chan), [wenfeng\\_xiao@163.com](mailto:wenfeng_xiao@163.com) (W.F. Xiao), [jun\\_li@rush.edu](mailto:jun_li@rush.edu) (J. Li), [delamoc@ccf.org](mailto:delamoc@ccf.org) (C.A. de la Motte), [jsandy44@gmail.com](mailto:jsandy44@gmail.com) (J.D. Sandy), [anna\\_plaas@rush.edu](mailto:anna_plaas@rush.edu) (A. Plaas).

*COL1A1*, *COL5A1*, *TIMP1*). In addition, other laboratories<sup>8–10</sup> also reported high expression of *COL1A1*, *COL2A1*, *COL3A1*, and *COL5A1* in human OA cartilages. Moreover, mice deficient in genes that enhance collagen matrix formation and turnover in wound healing (*Adams5*, *Ddr2*, *Mmp13*, *Sdc4*, and *Tgm2*<sup>11–14</sup>) were variably protected from surgically induced OA.

In dermal wound healing, early inflammation is followed by formation of granulation tissue containing progenitor cells embedded in a provisional extracellular matrix (ECM) of collagens, fibronectin, hyaluronan (HA), and hyalactans<sup>15</sup>. These cells, following re-epithelialization, mature into fibroblasts to generate the functional collagenous repair tissue. Correspondingly, following cartilage injury, proliferation of cells and ECM deposition in synovial lining and adjacent adipose or joint capsule tissues occurs. This response can progress into fibrotic remodeling, often reported in inflammatory arthritis<sup>16</sup>. A similar response also develops in the meniscal destabilization mouse model of OA, where, at 2–4 weeks<sup>17</sup>, an inflammatory period is followed by elevated expression of profibrotic mediators such as type III collagen (*Col3a1*), fibromodulin (*Fmod*, a catalyst for TGF- $\beta$ 1 signaling), and prolargin (*Prelp*, an inhibitor of osteoclastic activity).

To examine repair responses specifically in the context of articular cartilage injury, we have adapted a murine model induced by surgical excision of cartilage from the patellar groove<sup>18</sup>. This allowed spatiotemporal macroscopic and microscopic evaluation of whole joint-responses and assay of gene expression in inflammatory, pro-fibrotic and ECM pathways, in both intact joints and separated tissue pools (meniscus and synovium (Men/Syn), cartilage and subchondral bone (C/SCB), and patellar tendon (PT)).

We have also examined such injury responses in mice deficient in HA synthase 1 (*Has1*), which have previously been reported to exhibit an aberrant dermal healing phenotype<sup>19</sup>. We show that *Has1*<sup>-/-</sup> mice, although not defective in overall HA production, are not able to control post-injury joint inflammation and develop extensive intra-articular scarring and severe OA-like symptoms.

## Methods

### Murine cartilage injury model

Wild-type (WT) and *Has1*<sup>-/-</sup> male C57Bl/6 mice (10–12 weeks old, ~30 g) were used under approval of the Rush University Institutional Animal Care and Use Committee. Routinely, four C57Bl/6 males were caged with one C57Bl/6 female littermate, to minimize male aggression and prevent wounding in the pre-op and post-op maintenance periods. After anesthesia, an ~8-mm medial para-patellar incision was made on the right knee, medial para-patellar arthrotomy was performed, and the patella laterally luxated. Cartilage was debrided along the distal groove with a #15 scalpel without penetration of the subchondral bone. Joint surfaces were lavaged with sterile saline, and the patella repositioned, before the muscle layer and skin were closed with 6-0 Vicryl sutures. Supporting ligaments, menisci, and other cartilage surfaces were not damaged [Fig. S-1(A)], and no changes were detected in the contralateral joint post-injury [Fig. S-1(B)]. Sham surgery included all steps except cartilage debridement. Mice were maintained at cage activity during the 4-week post-surgery period. The minimal number of mice needed for each outcome was determined based on previous studies<sup>20</sup>, and the numbers in each experimental group are given (Table S-1).

### Macroscopic joint imaging, histology, and HA staining

Joint-wide pathology was assessed in operated and contralateral joints as previously described<sup>20</sup>. For histology, whole joints (after

removal of skin and muscle) were fixed in 10% neutral-buffered formalin, decalcified with 5% EDTA in PBS, paraffin-embedded, and microtome-cut into 6- $\mu$ m sections across the entire joint<sup>20</sup>. Sections 1–60, 61–120, and 121–190 spanned medial, central groove, and lateral compartments, respectively. Slides 1/2, 22/23, 42/43, 62/63, 82/83, 102/103, 122/123, 142/143 and 182/183 were stained with Safranin O (Safo), and adjacent sections with hematoxylin and eosin (H&E) or biotinylated HA binding protein (bHABP) to localize HA. It should be noted that the histological analysis was not used in this study to generate a numerical scale for cartilage grading (as per OARSI guidelines) but evaluated, in combination with the macro-images, to describe structural alterations in multiple tissue types adjacent to the injury and throughout the whole joint.

### Quantitative PCR (qPCR)

For gene expression in whole joints from naïve, sham, and injured groups ( $n = 3–4$ , detailed in Table S-1), hind legs were harvested immediately after sacrifice, the skin and muscle removed, and knee joints isolated by sharp dissection through the growth plates, prior to storage at  $-20^{\circ}\text{C}$  in RNAlater (Table S-1). To prepare separate tissue pools, twelve joints were used for Men/Syn or PT, and two for C/SCB. RNA purification, cDNA synthesis, and qPCR (3 technical replicates) with Taqman®-primers (Table S-2) was done as previously described<sup>20</sup>. Transcript abundance was calculated as  $1000 \times 2^{-\Delta\text{Ct}}$ , with  $\Delta\text{Ct} = [\text{Ct}(\text{gene of interest}) - \text{Ct}(\text{Gapdh})]$  and  $\text{Ct} > 35$  considered “non-detectable” (ND). RT<sup>2</sup> Profiler PCR Arrays (Qiagen) were used for fibrosis (PAMM-120ZA) and NF- $\kappa$ B signaling target (PAMM-225ZA) genes. Injury-induced fold-change in expression was calculated as  $2^{-\Delta\Delta\text{Ct}}$ , where  $\Delta\Delta\text{Ct} = [\Delta\text{Ct}(\text{post-injury time point}) - \Delta\text{Ct}(\text{naïve})]$ . Gene groupings indicated by Qiagen and Metacore™ software analysis of expression data were used to determine pathway associations.

### Data and statistical analysis

For statistical comparisons across time points and between genotypes, qPCR assays were performed on whole joints (each joint an experimental unit), from naïve, sham, and injury groups, because the large number of mice (12 per experimental unit) required for generating multiple pools of separated tissue types was outside the scope of this study.

*Gapdh* Ct values from WT and *Has1*<sup>-/-</sup> samples were pooled to confirm normality of Ct values with the Shapiro-Wilk test, and analysis of variance (ANOVA) was used to compare *Gapdh* Ct values across groups to confirm selection of the housekeeping gene. For all combinations of WT/*Has1*<sup>-/-</sup> naïve/sham/injury joints (6 in total), Ct values were confirmed with the Shapiro-Wilk test to be normally distributed. For each gene, ANOVAs were performed on  $\Delta\text{Ct}$  values to compare expression in the following subgroups: 1-way ANOVA for WT naïve vs 12 or 28 day post-sham; 2-way ANOVAs for WT vs *Has1*<sup>-/-</sup>, naïve vs 12 or 28 day post-injury (main effects: experimental end point, genotype). ANOVAs were followed by post hoc analysis of statistically significant effects using unpaired, two-tailed Student's *t* tests with Bonferroni correction of the *P* value for multiple comparisons against naïve. Since only two end points at biologically distinct phases of sham and injury response were compared to naïve, Bonferroni correction was chosen as the most conservative option for post hoc comparisons after ANOVA.

For each gene from the arrays, unpaired two-tailed Student's *t* tests were used to compare between WT and *Has1*<sup>-/-</sup>  $\Delta\text{Ct}$  values at naïve. Similar analysis was performed to compare array results of WT naïve to WT sham. ANOVA was used to compare genotypes for  $\Delta\text{Ct}$  values after injury (to determine the overall effect of genotype),

followed by a post hoc unpaired, two-tailed Student's *t* test with Bonferroni correction. The experiment-wide significance level was  $\alpha = 0.05$ .

## Results

### Macroscopic imaging of the murine model of cartilage injury in WT joints

Cartilage was debrided along the full length of the patellar groove without damaging the trochlear ridges [Fig. 1(A)] or subchondral bone. Typical images of joints at 4 weeks post-surgery [Fig. 1(B)] illustrate that the trochlear ridges adjacent to the injury-site were covered with a whitish tissue [Fig. 1(B), arrows] extending into the periosteum. Safo or H&E histology showed this to be dense fibrous tissue lacking chondroid staining and with few

cells (data not shown). The damaged groove surface became covered with a thin layer of tissue, but the apposing patellar cartilage was markedly roughened, with evidence of tissue ingrowth from the margins [Fig. 1(B)]. Contralateral joints remained macroscopically unaffected [Fig. S-1(B)], and sham operated joint surfaces also showed no damage after 4 weeks [Fig. S-1(C)].

### Histology of joint tissue responses to cartilage injury in WT mice

Typical images of Safo-stained whole joint sections from naïve and 1- and 4-weeks post-injury WT mice [Fig. 1(C)] show the cartilage interfaces between the proximal groove and the center of the patella (top panels) and between the distal groove and the distal patellar tendon (bottom panels). In naïve mice, these showed full-depth patellar cartilage in apposition to the groove cartilage,

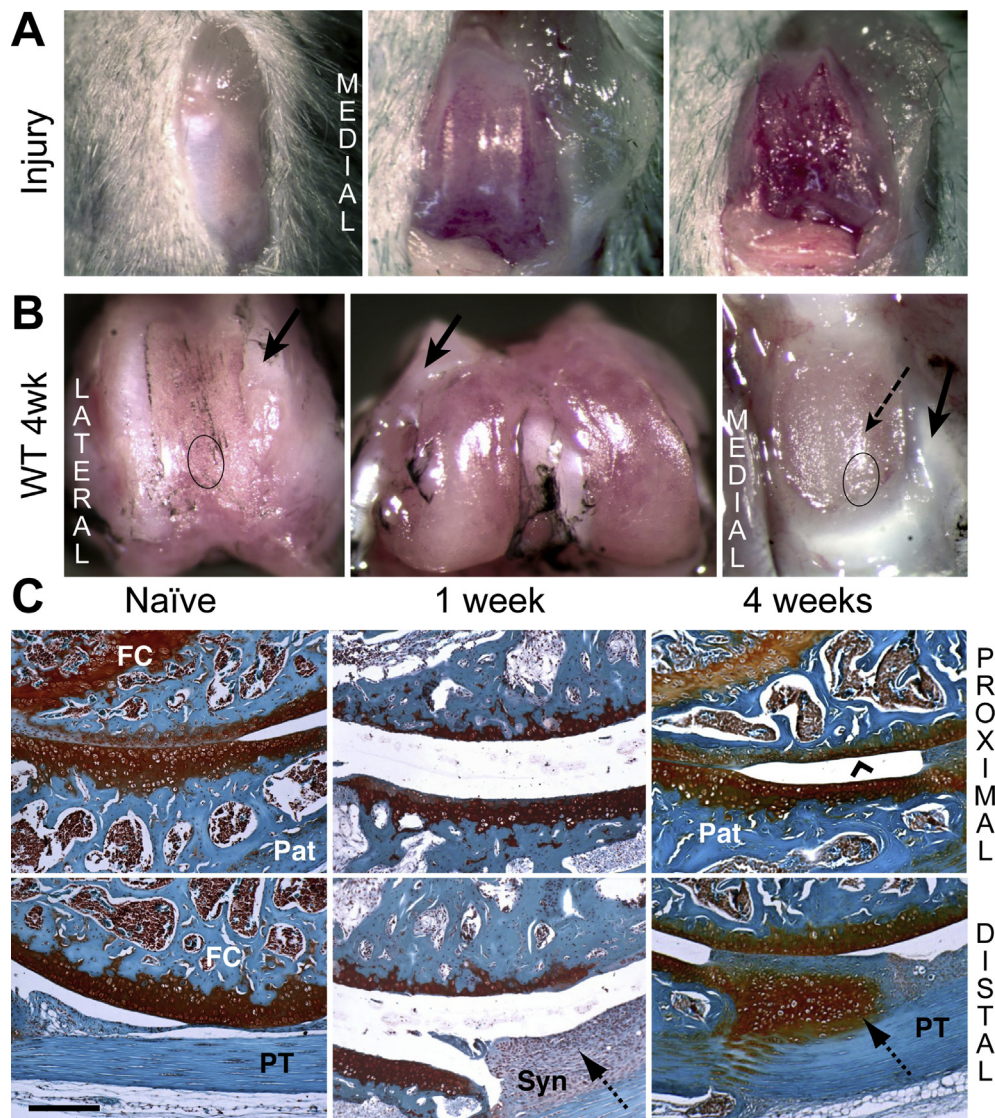


**Fig. 1. Macroscopic and histological evaluation of joint tissue response to cartilage injury in wild type mice.** A) The joint capsule was opened via medial peri-patellar incision, and cartilage debrided along the patellar groove of the right knee. B) The macroscopic appearance of cartilage surfaces and adjacent soft tissues was examined in the injured joint at 4 weeks post-surgery. Dense fibrous tissue formation (solid arrows) at the margins of the injured area and cartilage wear on the patella (dashed arrow) are indicated. C) Safranin-O staining of tissue structures in the femoral-patellar compartment of naïve joints and at 1 and 4 week post-injury permitted histological evaluation. The approximate regions of the groove and the patella taken for histology are indicated by circles in panel B. Cartilage resurfacing (chevron arrowhead) is observed on the femoral groove. The hyperplastic tissue deposition at the synovium (dotted arrows) at week 1 developed into a chondrophytic deposit by week 4. (Pat = patella; FC = femoral condyle; PT = patellar tendon; Syn = synovium). Scale bar = 100  $\mu$ m.



transitioning into a Safo-poor fibrous tissue at the proximal end. At 1 week post-injury, a thin layer of calcified cartilage, remaining after the debridement, covered the subchondral bone of the proximal groove [Fig. 1(C), upper panel]. The patellar cartilage apposing the injury site showed marked thinning relative to naïve, likely as a result of mechanical abrasion or degradative mediators released from the area of cartilage injury. Although subchondral bone was not penetrated, the cellularity in the marrow space of both bones was reduced at 1 week post-injury [Fig. 1(C)] and spaces filled with a disorganized ECM. A thick layer of hyperplastic synovium, extending between the patellar tendon and the distal patella was prominent at 1 week.

At 4 weeks, a continuous layer of Safo-stained “repair” cartilage covered the injured groove, and the cellularity of the marrow space had regenerated. The patellar cartilage surface was also restored, and all injured joints developed chondrophytic deposits with a fibrous covering [Fig. 1(C), lower panel] derived from the hyperplastic synovium adjacent to the patella. Hyperplasia of both peripatellar and perimeniscal synovium and the loss of adipocytes by 1 week was confirmed by H&E histology [Fig. 2(A)]. By 4 weeks, normal cellularity was restored with minor thickening of the perivascular matrix. A transient influx of neutrophils to vascularized regions at the dermal incision site was evident at 3 days post-surgery (data not shown), but no infiltration of circulating inflammatory cells into the synovium or the joint space was detected, consistent with only innate inflammation.

When equivalent sections were examined for HA deposition, strong staining of synovium was seen at 1 week [Fig. 2(B), left panel], but at 4 weeks HA staining essentially returned to naïve levels. The HA accumulation early post-injury is consistent with the increased expression of *Has1* ( $P < 0.01$ ) and *Has2* ( $P < 0.05$ ) at those times. *Has1* expression remained significantly elevated (12d:  $P < 0.01$ , 28d:  $P < 0.05$ ) at later times (Fig. S-3), suggesting that long-term ECM remodeling includes this prolonged expression response. Expression of *Has1* and *Has2* in contralateral joints was unaffected [Fig. S-3(A)]. Furthermore, sham-operated joints at 2 weeks

**Table 1**

Effect of cartilage injury on mRNA abundance relative to *Gapdh* of HA-network genes in isolated tissue pools from WT mice

	<i>Has1</i>	<i>Has2</i>	<i>Tnfrsf10b</i>	<i>Itih2</i>
<b>Naïve</b>				
Cartilage and subchondral bone	0.36	0.06	0.12	0.11
Meniscus and synovium	24.4	0.41	1.28	1.03
Patellar tendon	2.58	0.27	2.32	0.51
<b>1 week</b>				
Cartilage and subchondral bone	4.17 (12)*	0.06 (1.1)	1.75 (15)	0.04 (0.4)
Meniscus and synovium	78.5 (3.2)	2.83 (7.0)	55.6 (43)	1.91 (1.9)
Patellar tendon	33.9 (13)	2.68 (10)	51.2 (22)	0.65 (0.8)
<b>4 weeks</b>				
Cartilage and subchondral bone	3.73 (10)	0.03 (0.5)	1.06 (8.9)	0.08 (0.8)
Meniscus and synovium	54.6 (2.2)	0.40 (1.0)	10.4 (8.1)	1.92 (1.9)
Patellar tendon	44.2 (17)	1.19 (4.4)	18.2 (7.9)	3.90 (7.7)

\* Italicized numbers in parentheses are fold change relative to naïve levels.

showed only mild peri-patellar synovial hyperplasia, which resolved at 4 weeks (data not shown). Minor fibrotic/chondroid remodeling at the patellar margins was observed [Fig. S-1(C)], but femoral or tibial articular and growth plate cartilage appeared normal.

#### Post-injury expression of HA-matrix genes in WT joint tissues

Injury to skin<sup>21</sup>, intestine<sup>22</sup>, cartilage<sup>23</sup>, and other tissues is accompanied by inflammation and changes in HA accumulation, resulting from concurrent increased synthesis of HA itself and HA-associated proteins, such as TSG6 (encoded by *Tnfrsf10b*), the heavy chains of inter-alpha-trypsin inhibitor (encoded by *Itih1-5* genes), and pentraxin.

Increased expression of some of these genes also occurred after cartilage injury (Table 1). In naïve joints, all transcripts except for *Tnfrsf10b* were most abundant in the Men/Syn tissue pools, followed by PT and C/SCB pools, consistent with the staining intensity of HA

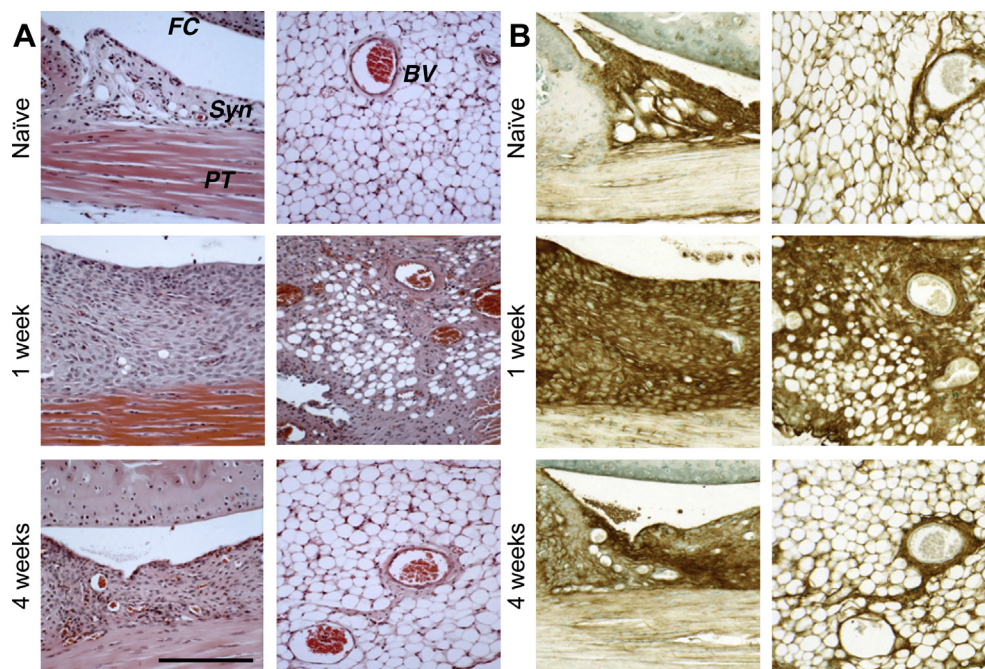


**Fig. 2. Histological evaluation of hyperplasia in peripatellar and perimeniscal synovium and adipose tissue following cartilage injury in wild type mice.** A) H&E staining showed post-injury cellular hyperplasia and increased ECM deposition at the synovial lining, in the adipose stroma, and perivascular regions. B) Sections equivalent to those shown in (A) were stained for HA using bHABP. (FC = femoral condyle; PT = patellar tendon; Syn = synovium; BV = blood vessel). Scale bars = 100  $\mu$ m.

**Table II**  
Effect of cartilage injury on mRNA abundance relative to *Gapdh* of ECM genes in separate tissue pools from WT mice

	<i>Acan</i>	<i>Vcan V1</i>	<i>Vcan V2</i>	<i>Col1a1</i>	<i>Col2a1</i>	<i>Col3a1</i>
<b>Naïve</b>						
Cartilage and subchondral bone	1.87	26.9	ND	1720	1.22	1.6
Meniscus and synovium	0.85	5.21	0.16	1280	0.15	24.6
Patellar tendon	0.04	6.33	0.05	962	ND	2.6
<b>1 week</b>						
Cartilage and subchondral bone	10.1 (5.4)*	12.7 (0.5)	0.47 (–)	3550 (2.1)	1.87 (1.5)	62.9 (39)
Meniscus and synovium	61.8 (72.3)	15.2 (2.9)	15.2 (92)	10,300 (8.0)	0.38 (2.6)	4010 (163)
Patellar tendon	130 (3386)	11.1 (1.8)	17.2 (366)	10,900 (11)	0.42 (–)	4451 (1734)
<b>4 weeks</b>						
Cartilage and subchondral bone	7.97 (4.3)	8.85 (0.3)	0.18 (–)	4880 (2.8)	1.38 (1.1)	54.8 (34)
Meniscus and synovium	8.12 (9.5)	2.80 (0.5)	1.75 (10.6)	2770 (2.2)	0.80 (5.4)	1080 (44)
Patellar tendon	83.7 (2180)	6.87 (1.1)	4.41 (94)	7380 (7.7)	17.7 (–)	3200 (1245)

\* Italicized numbers in parentheses are fold change relative to naïve levels. ND = not detected (Ct > 35), with no fold change calculation possible (–).

[Fig. 2(B)]. At 1 week, *Has1* expression increased markedly in all tissues and remained elevated at 4 weeks. *Has2* was also increased at 1 week in the Men/Syn and PT, remaining elevated in PT up to 4 weeks but normalizing in the Men/Syn (Table I). Concurrent with the increased expression of *Has1* and *Has2*, *Tnfrsf11b* was activated at 1 week in all tissues, particularly in Men/Syn (43-fold) and PT (22-fold). Expression levels declined, but did not normalize, by 4 weeks. *Itih2* expression was minimally affected in all tissues at both time points, except for a 7.7-fold increase in the PT at 4 weeks. *Itih1* expression was virtually undetectable in any samples (data not shown).

#### Post-injury changes to expression of ECM genes in WT tissues

We also assayed for changes in several ECM-related genes known to be associated with matrix remodeling in cartilaginous and fibrous tissue in individual tissue pools (Table II). In naïve tissues, transcripts for *Acan*, *Vcan V1* (formerly named the *V0* isoform), and *Col2a1* were highest in the C/SCB, and for *Col3a1* in the Men/Syn. Notably, *Col1a1* transcripts were very high relative to other genes in the three tissue pools, and *Vcan V2* (formerly *V1*) was barely detectable.

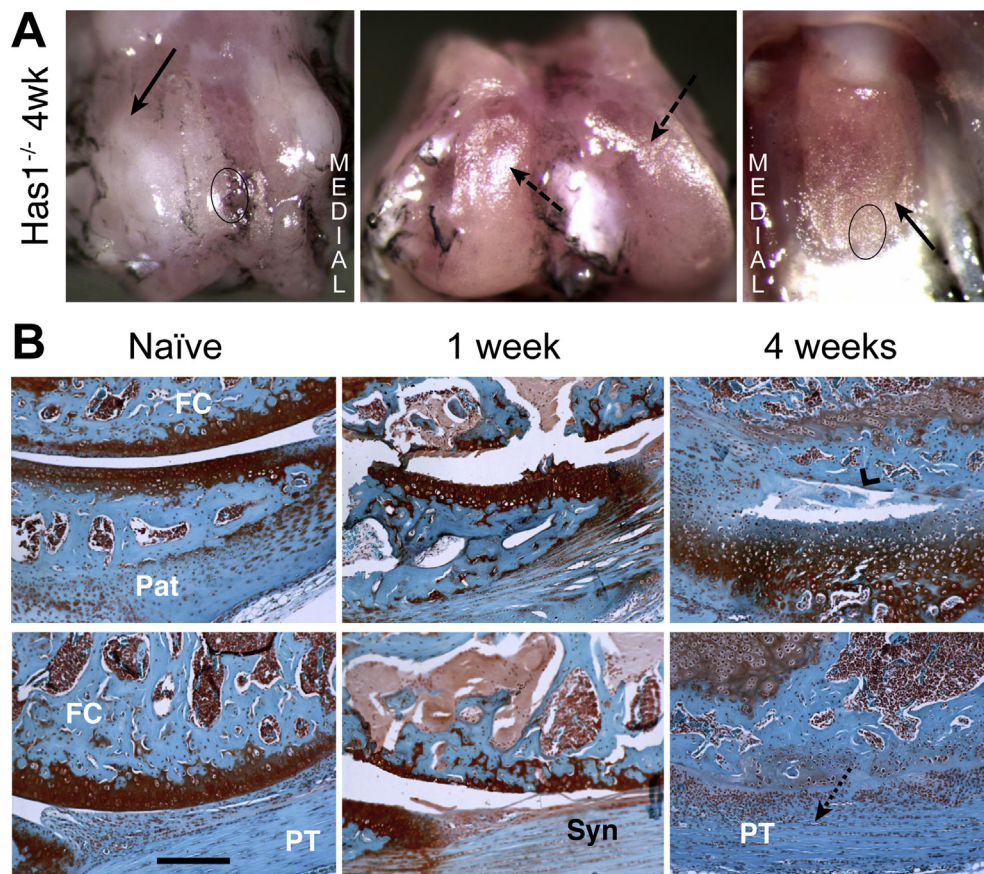


**Fig. 3. Macroscopic and histological evaluation of joint tissue response to cartilage injury in *Has1*<sup>-/-</sup> mice.** A) The macroscopic appearance of cartilage surfaces and adjacent soft tissues in the injured joint was examined at 4 weeks post-surgery. Extensive fibrotic deposits (solid arrow) were observed at the groove, and both the condylar and patellar cartilage showed signs of wear (dashed arrows). B) Sections from the femoral-patellar compartment of naïve joints and at 1 and 4 weeks post-injury were stained with Safranin-O. The approximate region of the groove and the patella taken for histology are indicated by circles in panel B. By 4 weeks post-injury, severe cartilage and bone loss (chevron arrowhead) combined with extensive fibrotic overgrowth (dotted arrow) results in a loss of joint space. (Pat = patella; FC = femoral condyle; PT = patellar tendon; Syn = synovium). Scale bar = 100  $\mu$ m.



All genes were increased at 1 week post-injury, with the increases both tissue- and gene-specific. Increases in expression were highest for *Acan*, *Vcan* V2, and *Col3a1* in the PT, possibly induced by manipulation at the time of surgery and through its proximity to the reactive synovium (Figs. 1 and 2). In contrast, expression of assayed genes was minimally affected in C/SCB. At 4 weeks post-injury, expression in Men/Syn and C/SCB decreased markedly to near naïve levels, but there was continued elevation of *Acan*, *Vcan* V2, and *Col3a1* in the PT.

#### Gene expression in contralateral and sham-operated joints

A selected group of genes was assayed in contralateral and sham operated joints (Fig. S-3). Expression was essentially unaffected in contralateral tissues, consistent with minimal systemic post-injury responses. In sham-operated joints, there was a significant increase in expression of *Has1*, *Tnfrsf11b* and *Col3a1* by 12 days, similar to that in fully injured joints. All genes returned to naïve levels in the sham by 28 days, except for *Has1* and *Col3a1*, which both remained elevated, suggesting that these are specific indicators of joint damage itself.

#### *Has1* ablation modifies joint tissue response to cartilage injury

Since *Has1* was highly activated and sustained after cartilage injury (Table 1) and given the importance of HA in connective tissue healing, we examined cartilage injury responses in *Has1*<sup>-/-</sup> joints. Macroscopic examination of *Has1*<sup>-/-</sup> joints at 4 weeks post-injury [Fig. 3(A)] showed a dense collagenous tissue covering of the trochlear ridges and extending to the adjacent periosteum, whereas this was not seen in the WT [Fig. 1(B)]. Instead of the partial regeneration

of cartilage seen in WT joints, widespread damage to the cartilage and subchondral bone was seen [Fig. 3(B)] at 1 week, with extensive fibrotic overgrowth (devoid of any Safo staining) developing in these areas [Fig. 3(B)]. Most notable was the finding that, at 4 weeks, the fibrotic tissue expanded from the injury site [Fig. 3(B)] into all soft tissues and also filled and thus eliminated the joint space.

*Has1* deficiency did not affect HA deposition at 1 week or its decrease at 4 weeks seen in the synovial lining, adherent adipose tissue, and SCB marrow (Fig. 4). This is consistent with the accepted notion that HAS2, but not HAS1 or HAS3, is the primary HA-producing synthase throughout all organs<sup>24</sup>, and therefore also responsible for the increased HA deposition seen in both the WT and *Has1*<sup>-/-</sup> joints.

The tissue-specific and temporal post-injury gene expression trends (Table S-3) were similar for WT and *Has1*<sup>-/-</sup> mice, with transcripts for *Has3* and *Itih1* undetectable in both strains; however, there were significant differences between genotypes with time (Fig. 5). In WTs, *Col2a1* ( $P < 0.05$ ) expression decreased at day 3 and returned to naïve levels by day 12, whereas expression of *Has1* ( $P < 0.01$ ), *Has2* ( $P < 0.001$ ), and *Tnfrsf11b* ( $P < 0.01$ ) increased at 3 days and remained increased at 12 days (Figs. 5 and S-4). Expression of *Col1a1* ( $P < 0.05$ ) and *Col3a1* ( $P < 0.001$ ) peaked at day 12, and *Col1a1*, but not *Col3a1* ( $P < 0.05$ ), returned to naïve levels by day 28 (Fig. 5). WT joints showed an increased expression of HA-matrix genes up to 12 days and a sustained increase of *Col3a1* up to 28 days. In summary, whereas *Has1*<sup>-/-</sup> joints responded post-injury like WT for matrix genes, they did not show as clear a normalization of HA-matrix genes at later times.

Only in *Has1*<sup>-/-</sup> joints was *Col1a1* ( $P < 0.01$ ) inhibited at 3 days and *Vcan* V2 ( $P < 0.05$ ) activated at 28 days (Fig. 5). Although

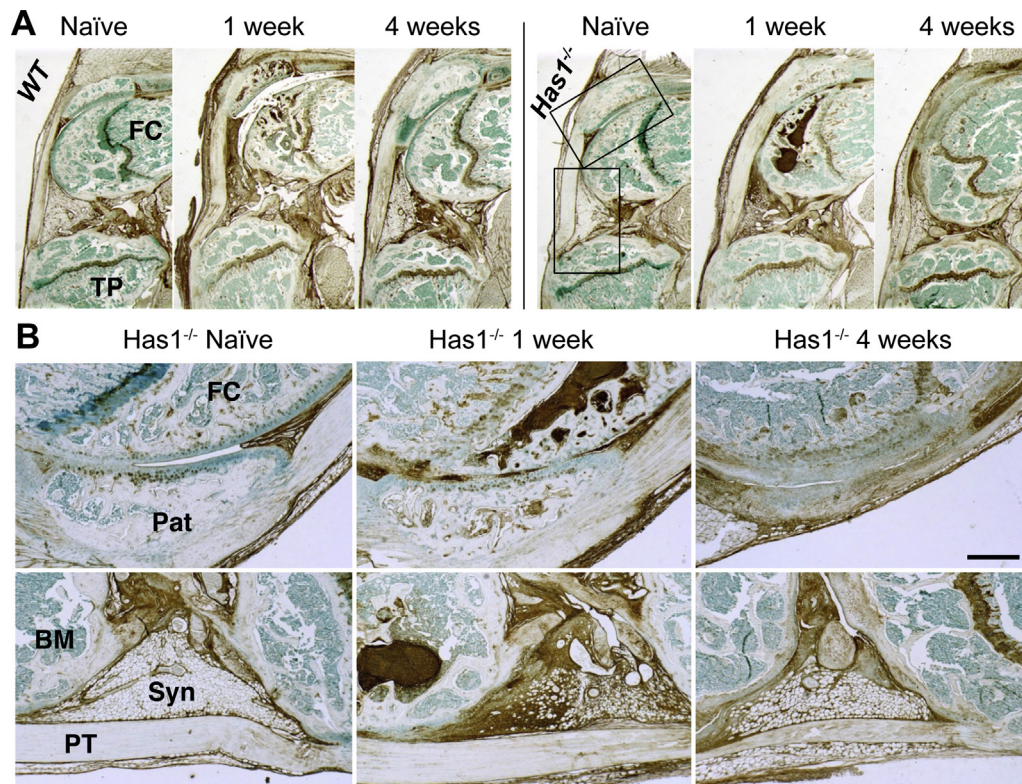


**Fig. 4.** Histological evaluation of HA distribution in naïve and post-injury joint tissues of WT and *Has1*<sup>-/-</sup> mice. A) Sagittal sections stained with bHABP are shown at low magnification. B) High magnification images of patella/patellar groove/peri-patellar synovium (upper panel) and peri-menisal adipose tissue (lower panel) from *Has1*<sup>-/-</sup> joints (see boxed areas in (A)) show the prominent increase in HA deposition in post-injury joints. (Pat = patella; FC = femoral condyle; TP = tibial plateau; PT = patellar tendon; Syn = synovium; BM = bone marrow) Scale bar = 100  $\mu$ m.

temporal trends for HA-matrix genes were mostly similar to WT, *Has1*<sup>-/-</sup> joints showed no significant changes with injury in *Has2* and *Tnfaip6* expression (Fig. 5). Thus, *Has1* ablation was accompanied by a lower trend in activation of *Has2* expression at 3 days, a much greater stimulation of *Tnfaip6* at 12 days ( $P < 0.01$ ), and a significant activation of *Itih2* expression ( $P < 0.05$ ) at 12 days, indicating that its effects are not on HA production itself but on the genes associated with forming the HA matrix.

#### Effect of *Has1* ablation on gene pathway changes at different periods after injury

The lack of cartilage regeneration, degenerative changes on adjacent cartilage surfaces, and extensive fibrotic remodeling of the synovium and joint capsule in *Has1*<sup>-/-</sup> mice are consistent with development of a chronic inflammatory environment in the post-injury joint. To establish a possible link between chronic inflammation and post-injury fibrotic scarring, we analyzed joints from both genotypes for NF- $\kappa$ B signaling target and fibrosis genes. Assays were done for naïve and 12- or 28-days post-injury in both genotypes, and data calculated as fold-change relative to genotype naïve (Tables S-6 and S-7). Notably, compared to WT, *Has1*<sup>-/-</sup> mice over-

expressed a larger number (26 genes at >3 fold) of the NF- $\kappa$ B signaling target genes (Table S-4) and fibrosis genes (Table S-5).

Pathway associations were determined for genes that were modified at least 3-fold relative to naïve levels using Metacore™ software. For both genotypes, four functional gene groupings were identified: IL-17/IL-6 signaling, ECM remodeling, pro-apoptosis, and anti-apoptosis (Table III). Moreover, within those groups, there were differences between WT and *Has1*<sup>-/-</sup> in expression of many genes, with 27 showing 6-fold or greater differences between WT and *Has1*<sup>-/-</sup> (Table III): for IL-17/IL-6 signaling, *Csf3*, *Map2k6* (12 days) and *Cxcl1*, *Il6*, *Mmp1a*, *Ptgs2* (28 days); for ECM remodeling, *Col1a2* ( $P < 0.01$ ), *Ctgf* ( $P < 0.05$ ), *Timp2* (12 days) and *Plat*, *Serpine1*, *Tgfb3*, *Thbs2*, *Timp1* (28 days); for pro-apoptosis genes, *Fasl*, *Ifng*, *Il4*, *Ins2* ( $P < 0.01$ ), *Lta* (12 days) and *Il4*, *Ins2*, *Tnfsf10*, *Traf2* (28 days); and, for anti-apoptosis genes, *Birc3*, *Cd40*, *Csf2*, *Fas*, *Il2*, *Rela* (12 days) and *Csf2* (28 days).

#### Discussion

Repair of articular cartilage defects in human joints remains problematic despite extensive research, due in part to insufficient information on self-healing mechanisms after injury. To mimic the

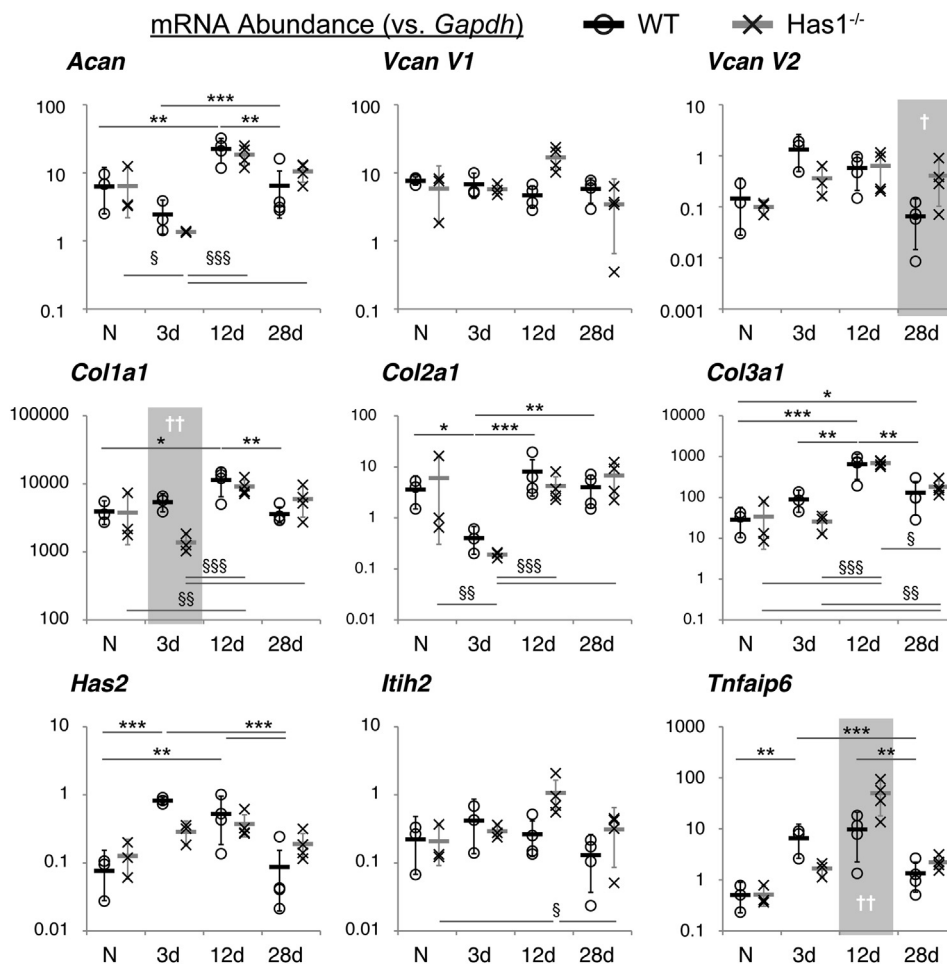


**Fig. 5.** Expression of selected ECM and HA network genes in WT and *Has1*<sup>-/-</sup> joints. Gene expression, calculated as mRNA abundance relative to *Gapdh* (see Methods), of WT (circles) and *Has1*<sup>-/-</sup> (crosses) whole joints at each time point (naïve (N) & 3d:  $n = 3$ ; 12d & 28d:  $n = 4$ ) is shown for each biological replicate. Means within each group are shown as a thick black or gray bar, and the error bars represent the transformed upper and lower bounds of a 95% confidence interval for the two genotypes at each time point. Statistical significance between time points, after two-way ANOVA and correction for multiple comparisons (see Methods), at  $P < 0.05$  (\*),  $P < 0.01$  (\*\*/§§), and  $P < 0.001$  (\*\*\*/§§§), between time points are indicated for WT/*Has1*<sup>-/-</sup> joint gene expression. Statistically significant differences between genotypes are indicated for  $P < 0.05$  (†) and  $P < 0.01$  (††) and highlighted with a gray area.

focal cartilage defects commonly seen in highly active populations like athletes<sup>1</sup> and the military<sup>25</sup>, we have used a non-bleeding, cartilage-only injury model to confine the repair response to factors from within the joint and minimize the role of cell infiltration from the circulation or the bone marrow.

Acute post-injury synovitis, peripatellar chondrocytes, and joint capsule fibrosis seen in this model have not been reported for other widely used models of murine OA<sup>26</sup>. This might be due to more severe responses to a cartilage injury or a reduced focus on the anterior joint compartment in other studies. In murine OA models, the focus is often on loss of cartilage of the tibiofemoral interface as observed on histology of coronal sections of the joint, while excluding examination of the anterior joint compartment, where severe changes in the synovium and joint capsule were seen in the present study, using sagittal sections. A unique effect of cartilage injury on joint response is suggested by the finding that, with the exception of *Col3a1* and *Mmp3* activation, structural and metabolic responses in the DMM model<sup>17</sup> are distinct from those in

the current work, suggesting pathogenesis of murine and likely human OA is dependent on type and severity of tissue injury, as well as mechanical perturbations.

A mechanistic link among inflammation, intra-articular scarring, and poor joint repair is also evident in this study, as we identified 27 genes related to IL-17/IL-6, ECM remodeling, and apoptosis (Table III) with higher expression in *Has1<sup>-/-</sup>* joints. To determine whether these are linked to the pathology of *Has1<sup>-/-</sup>* joints, we researched whether they have previously been implicated in poor repair of connective tissue injury, using murine OA as reference. On the basis of this restricted search, we have concluded that the 27 genes identified are indeed good markers of ineffective joint repair.

With regard to genes related to IL-17/IL-6 pathways, IL-17 is highly linked to OA in a transcriptomic study of human hip cartilages<sup>10</sup> and correlated with collagen expression in scleroderma and fibrosis<sup>27</sup>. The IL-17/IL-6 pathway genes found differentially activated here are increased in inflammation and fibrosis. *Csf3* and

**Table III**  
Effect of cartilage injury in multiple genes related to NF-κB signaling targets and fibrosis in whole joint preparations from WT and *Has1<sup>-/-</sup>* mice

IL-17/IL-6 signaling	WT (12d)	<i>Has1<sup>-/-</sup></i> (12d)	WT (28d)	<i>Has1<sup>-/-</sup></i> (28d)	ECM remodeling	WT (12d)	<i>Has1<sup>-/-</sup></i> (12d)	WT (28d)	<i>Has1<sup>-/-</sup></i> (28d)
<i>Akt1</i>	↓	+	↓	↓	<i>Bmp7</i>	↓↓↓	↓	↓↓	↓
<i>Ccl3</i>	↓↓↓	↓↓*	↓	+	<i>Col1a2</i>	↓↓	+¶**	↓	↔
<i>Ccl11</i>	+	↔	+	++	<i>Col3a1</i>	+++	++++	++	+++
<i>Ccr2</i>	↓↓	↓↓↓	↓	↓	<i>Ctgf</i>	↓↓	+¶*	↓	↔
<i>Cebpb</i>	↓↓↓	↓	↓↓↓	↓↓	<i>Egf</i>	↓	+	↓	↓
<i>Csf2rb</i>	++	+++	++	++	<i>Egfr</i>	++	+++	↓	↔
<i>Csf3</i>	↓↓	+¶¶¶	↓	↓	<i>Grem1</i>	↓↓↓	↓↓*	↓↓	↓↓↓
<i>Cxcl1</i>	++	+¶¶¶	↔	+¶¶¶¶	<i>Lox</i>	+	+	↓	+
<i>Icam1</i>	↔	++	↓	+	<i>Mmp2</i>	++	+++	+	++
<i>Il1a</i>	↓↓	↔	↓	+	<i>Mmp8</i>	↓↓	↓↓	↓	↓
<i>Il1b</i>	↓↓	↓	↓	↓	<i>Mmp13</i>	↓↓	↓	↓	↓
<i>Il6</i>	+++	+¶¶¶	+	+¶¶¶¶	<i>Mmp14</i>	+	++	↓	+
<i>Il10</i>	↓↓	↓	+	↓	<i>Plat</i>	++	++	↓	+¶¶
<i>Jun</i>	+	+	↓	+	<i>Plau</i>	+	↓	↓	↓
<i>Map2k6</i>	↓	+¶¶	↓	+	<i>Plg</i>	↓	+	↓	+
<i>Mmp1a</i>	↓↓↓	↓↓↓	↓↓↓	+¶	<i>Serpina1a</i>	↓↓	↓↓	↓↓	↓↓
<i>Mmp3</i>	+¶¶¶¶	+¶¶¶¶	+¶¶¶¶	+¶¶¶¶	<i>Serpine1</i>	++	+++	+	+¶¶¶
<i>Mmp9</i>	↓	+	↓	+	<i>Serpinh1</i>	+	++	↓	+
<i>Nfkb1</i>	↓	+	↓	+	<i>Tgfb3</i>	+++	+¶¶¶	+	+¶¶¶¶
<i>Nfkbia</i>	↓	+	+	++	<i>Thbs2</i>	+++	+¶¶¶	+	+¶¶¶¶
<i>Ptgs2</i>	+++	+++	↓	+¶¶¶	<i>Timp1</i>	+	++	+	+¶¶¶+¶
<i>Rel</i>	↓	↓	↓	+	<i>Timp2</i>	++	+¶¶¶¶	↔	++
<i>Selp</i>	+++	+++	+++	+¶¶¶	<i>Timp3</i>	+	+	↓	+
<i>Sp1</i>	↓	↔	↓	↓	<i>Timp4</i>	↓↓↓	↓	↓↓	↓
Pro apoptosis	WT (12d)	<i>Has1<sup>-/-</sup></i> (12d)	WT (28d)	<i>Has1<sup>-/-</sup></i> (28d)	Anti-apoptosis	WT (12d)	<i>Has1<sup>-/-</sup></i> (12d)	WT (28d)	<i>Has1<sup>-/-</sup></i> (28d)
<i>Agt</i>	↓↓	↓	↓↓	↓	<i>Adm</i>	+	+++	↓	+
<i>Birc2</i>	↓	+	↓	↓	<i>Bcl2</i>	↓↓	↓	↓↓	↓
<i>Cd74</i>	↓	+	↓	↓↓	<i>Bcl2a1a</i>	↓	+	↓	↓
<i>Fasl</i>	↓↓	+¶¶	↓	+	<i>Bcl2l1</i>	↓↓	++	↓	↓
<i>Gadd45b</i>	++	++	↓	+	<i>Birc3</i>	↓	+¶¶	↓	↓
<i>Ifnb1</i>	↓↓↓	+	↓↓	↓	<i>Ccl12</i>	+	++	+	+
<i>Ifnγ</i>	↓↓	+¶¶	↓↓	↓	<i>Cd40</i>	↓	+¶¶	↓	↓
<i>Il12b</i>	↔	+	↓	↓	<i>Cdkn1a</i>	+	++	↓	↔
<i>Il2ra</i>	↓	+	+	+	<i>Csf2</i>	↓↓↓	+¶¶	↓↓	↔¶
<i>Il4</i>	↓↓	+¶¶	↓	+¶¶¶	<i>F3</i>	+	++	↓	+
<i>Ins2</i>	↓↓↓	+¶*	↓↓	+¶	<i>Fas</i>	↓	+¶¶	↓	+
<i>Irf1</i>	↓	+	↓	↓	<i>Il2</i>	↓↓↓	+¶	↓↓	↓
<i>Lta</i>	↓↓	+¶¶	↓	↔	<i>Myd88</i>	↓	+	↓↓	+
<i>Mitf</i>	↔	++	↓	+	<i>Nfkb2</i>	+	++	↓	+
<i>Myc</i>	↓	+	+	+	<i>Rela</i>	↓	+¶¶	↔	+
<i>Nqo1</i>	↓	+	↔	+	<i>Relb</i>	+	++	↓	↔
<i>Nr4a2</i>	+++	+¶¶¶	+	+¶¶	<i>Sod2</i>	↔	+	↔	+
<i>Stat1</i>	↓	↓	↓	+	<i>Stat5b</i>	+	++	+	+
<i>Tnfsf10</i>	↓	+	↓	+¶¶	<i>Tnf</i>	↓	↓	↓	+
<i>Traf2</i>	↓	+	↓	+¶¶	<i>Tnfrsf1b</i>	↓	↔	↓	+
<i>Trp53</i>	↓	+	↔	+	<i>Xiap</i>	↓	+	↔	+

**KEY:** Increase/decrease by < 2(+/-), 2–4 (++/↓↓), 4–8 (+++/↓↓↓), 8–16 (+++/↓↓↓), or 16+ (+++/↓↓↓) fold vs genotype naïve. No change (↔). >6-fold differential between genotypes (¶). Significant differences between genotypes (\*P < 0.05, \*\*P < 0.01).



*Map2k6* promote inflammation in dermal repair<sup>28</sup> and collagen-induced arthritis<sup>29</sup>, and *Il-6* is central for development of keloid disease<sup>30,31</sup>. *Mmp1a* is upregulated in inflammatory ischemia<sup>32</sup>, *Cxcl1* is a central inflammatory mediator in murine colitis<sup>33</sup>, and *Ptgs2* is highly expressed in the inflammatory phase of murine experimental OA<sup>34</sup>.

Of the ECM-remodeling genes, the notably elevated *Col1a1* and *Col1a2* expression in injured *Has1*<sup>-/-</sup> joints supports the non-reparative fibrotic scarring response, which appears to arise in progenitor-cell rich tissues such as synovium and periosteum, and the histological resemblance to hypertrophic scar tissue seen in keloid disease<sup>31</sup>. *Ctgf* expression is high in murine dermal sclerosis, but requires activation by IL-17<sup>35</sup>. The finding that *Timp2* and *Plat* are upregulated in the *Has1*<sup>-/-</sup> joint appears to be inconsistent with the findings that they have shown protection in knockout studies<sup>36,37</sup>. It is difficult to reconcile the *Timp2* observations; however, the *Plat* difference could be explained by the simultaneous enhancement of *Serpine1* (Table III), an inhibitor of *Plat*. Enhanced expression of *Tgfb3* occurs in experimental OA and is found in areas of osteophyte formation<sup>38</sup>. In a similar fashion, increased *Thsp2* expression is linked to chondrocyte formation, since it stimulates chondrogenesis in a rabbit osteochondral defect model<sup>39</sup>. Finally, the increased expression of *Timp1* expression in the *Has1*<sup>-/-</sup> mice is consistent with an increase in fibrous matrix deposition, since *Timp1* activation also occurs in the anabolic phase of a murine model of OA when ECM genes, including *Col1a1* and *Col5a1*, are also highly activated<sup>7</sup>.

The distinct elevated expression of apoptosis genes in *Has1*<sup>-/-</sup> joints (relative to WT) is consistent with an altered stress-induced apoptotic response in fibroblasts from *Has1*<sup>-/-</sup> and *Has3*<sup>-/-</sup> mice<sup>40</sup>. Moreover, *Has1*<sup>-/-</sup> joints showed elevated expression of *Il4* (Table III), a known stimulator of synovial fibrosis and fibroblasts-to-myofibroblast transition<sup>41</sup>. Elevated *Lta* (TNF $\beta$ ) expression results in an increased inflammatory response<sup>42</sup>, and increased *Ins2* expression has been linked to enhanced collagen deposition in muscle repair after injury<sup>43</sup>. Lastly, increases in *Ifng* and *Il2* expression are consistent with the findings that their joint fluid levels increase with OA severity<sup>44</sup> and that there is cross-talk between IFN- $\gamma$  and TGF- $\beta$  in dermal wound healing<sup>45</sup>. Lastly, an increase in *Rela* would allow for a higher expression of *Adamts5*, which has been linked to fibrotic scarring in murine OA<sup>46</sup>.

The apparently normal content of HA in naïve and injured *Has1*<sup>-/-</sup> joints suggests that HAS1 is not responsible for the synthesis of the “bulk” HA. However, a more limited activation of *Has2* expression in *Has1*<sup>-/-</sup> post-injury joints indicates that HAS1 may regulate HAS2 levels during the wound healing process. Moreover the absence of *Has1* could abrogate the activation of anti-inflammatory phagocytic cells, as evidenced by the decrease in pro-inflammatory cells and improvement of collagen fiber orientation observed with lentiviral over-expression of HAS1 in dermal repair<sup>47</sup>. Further, since HAS1 activity has been shown to be regulated by glucose concentration and several cytokines<sup>48,49</sup> during wound healing, it may synthesize a pericellular HA pool that controls mesenchymal cell fates in a post-injury environment<sup>19</sup> (Figs. 1, 2 and 4).

A link between inflammation and OA, particularly after injury, is well-documented<sup>50</sup>. However, mechanisms by which inflammation becomes chronic without the obvious presence of inflammatory cells in the joint remains to be established. The linkage between persistent activation of the NF- $\kappa$ B pathway, the excessive deposition of fibrotic scar tissue, and the chronic cartilage damage in injured *Has1*<sup>-/-</sup> joints may provide a novel model in which to study the interplay of these pathways in the pathogenesis of injury-induced OA.

## Contributions

DDC – contributed to experimental design and carried out murine surgeries, gene expression analyses, data evaluation, and manuscript preparation.

WFX – carried out murine surgeries, genotypic characterizing, and maintenance of *Has1*<sup>-/-</sup> mouse colony.

JL – carried out murine surgeries, maintenance of all mouse colonies, macroscopic imaging, and histology.

CdIM – consulted for experimental design and provided assistance with interpretation of HA histology and gene array data.

JDS – contributed to experimental design, data evaluation, and manuscript preparation.

AP – directed experimental design, data interpretation, and manuscript preparation.

AP ([anna\\_plaas@rush.edu](mailto:anna_plaas@rush.edu)) takes responsibility for the integrity of the work as a whole, from inception to finished article.

## Role of the funding source

Funding for authors include NIH (R01-AR057066; AP, WX, JL, JDS), the Arthritis Foundation (DDC), Seikagaku Corporation (DCC, JL) and the Katz-Rubschlager Endowment for OA Research (AP). These funding sources had no involvement in the study design, the data collection, analysis, and interpretation, the writing of this manuscript, and the decision to submit this work for publication.

## Competing interest statement

The authors have no conflicts of interest, perceived or actual, to declare.

## Acknowledgments

We acknowledge the help of Dr Zarema Arbieva of the University of Illinois at Chicago Genomics Core Facility for training and Katie Trella for assistance in the use of Metacore™-based gene array analyses. We also thank Dr Guanghua Lei for assistance in murine surgeries and Dr Katalin Mikecz for evaluating histological sections for inflammatory cell presence.

## Supplementary data

Supplementary data related to this article can be found at <http://dx.doi.org/10.1016/j.joca.2015.06.021>.

## References

- Flanigan DC, Harris JD, Trinh TQ, Siston RA, Brophy RH. Prevalence of chondral defects in athletes' knees: a systematic review. *Med Sci Sports Exerc* 2010;42:1795–801.
- Mashoof AA, Scholl MD, Lahav A, Greis PE, Burks RT. Osteochondral injury to the mid-lateral weight-bearing portion of the lateral femoral condyle associated with patella dislocation. *Arthroscopy* 2005;21:228–32.
- Buckwalter JA, Anderson DD, Brown TD, Tochigi Y, Martin JA. The roles of mechanical stresses in the pathogenesis of osteoarthritis: implications for treatment of joint injuries. *Cartilage* 2013;4:286–94.
- Liu-Bryan R. Synovium and the innate inflammatory network in osteoarthritis progression. *Curr Rheumatol Rep* 2013;15:323.
- Candela ME, Yasuhara R, Iwamoto M, Enomoto-Iwamoto M. Resident mesenchymal progenitors of articular cartilage. *Matrix Biol* 2014;39:44–9.
- Campbell TM, Trudel G, Wong KK, Laneville O. Genome-wide gene expression analysis of the posterior capsule in patients

- with osteoarthritis and knee flexion contracture. *J Rheumatol* 2014;41:2232–9.
7. Remst DF, Blom AB, Vitters EL, Bank RA, van den Berg WB, Blaney Davidson EN, et al. Gene expression analysis of murine and human osteoarthritis synovium reveals elevation of transforming growth factor beta-responsive genes in osteoarthritis-related fibrosis. *Arthritis Rheumatol* 2014;66:647–56.
  8. Aigner T, Fundel K, Saas J, Gebhard PM, Haag J, Weiss T, et al. Large-scale gene expression profiling reveals major pathogenic pathways of cartilage degeneration in osteoarthritis. *Arthritis Rheum* 2006;54:3533–44.
  9. Brew CJ, Clegg PD, Boot-Handford RP, Andrew JG, Hardingham T. Gene expression in human chondrocytes in late osteoarthritis is changed in both fibrillated and intact cartilage without evidence of generalised chondrocyte hypertrophy. *Ann Rheum Dis* 2010;69:234–40.
  10. Xu Y, Barter MJ, Swan DC, Rankin KS, Rowan AD, Santibanez-Koref M, et al. Identification of the pathogenic pathways in osteoarthritic hip cartilage: commonality and discord between hip and knee OA. *Osteoarthritis Cartilage* 2012;20:1029–38.
  11. Echtermeyer F, Bertrand J, Dreier R, Meinecke I, Neugebauer K, Fuerst M, et al. Syndecan-4 regulates ADAMTS-5 activation and cartilage breakdown in osteoarthritis. *Nat Med* 2009;15:1072–6.
  12. Little CB, Barai A, Burkhardt D, Smith SM, Fosang AJ, Werb Z, et al. Matrix metalloproteinase 13-deficient mice are resistant to osteoarthritic cartilage erosion but not chondrocyte hypertrophy or osteophyte development. *Arthritis Rheum* 2009;60:3723–33.
  13. Orlandi A, Oliva F, Taurisano G, Candi E, Di Lascio A, Melino G, et al. Transglutaminase-2 differently regulates cartilage destruction and osteophyte formation in a surgical model of osteoarthritis. *Amino Acids* 2009;36:755–63.
  14. Xu L, Servais J, Polur I, Kim D, Lee PL, Chung K, et al. Attenuation of osteoarthritis progression by reduction of discoidin domain receptor 2 in mice. *Arthritis Rheum* 2010;62:2736–44.
  15. Schultz GS, Wysocki A. Interactions between extracellular matrix and growth factors in wound healing. *Wound Repair Regen* 2009;17:153–62.
  16. Steenvoorden MM, Tolboom TC, van der Pluijm G, Lowik C, Visser CP, DeGroot J, et al. Transition of healthy to diseased synovial tissue in rheumatoid arthritis is associated with gain of mesenchymal/fibrotic characteristics. *Arthritis Res Ther* 2006;8:R165.
  17. Loeser RF, Olex AL, McNulty MA, Carlson CS, Callahan M, Ferguson C, et al. Disease progression and phasic changes in gene expression in a mouse model of osteoarthritis. *PLoS One* 2013;8:e54633.
  18. Eltawil NM, De Bari C, Achan P, Pitzalis C, Dell'Accio F. A novel in vivo murine model of cartilage regeneration. Age and strain-dependent outcome after joint surface injury. *Osteoarthritis Cartilage* 2009;17:695–704.
  19. Mack JA, Feldman RJ, Itano N, Kimata K, Lauer M, Hascall VC, et al. Enhanced inflammation and accelerated wound closure following tetraborborol ester application or full-thickness wounding in mice lacking hyaluronan synthases Has1 and Has3. *J Invest Dermatol* 2012;132:198–207.
  20. Li J, Gorski DJ, Anemaet W, Velasco J, Takeuchi J, Sandy JD, et al. Hyaluronan injection in murine osteoarthritis prevents TGFbeta 1-induced synovial neovascularization and fibrosis and maintains articular cartilage integrity by a CD44-dependent mechanism. *Arthritis Res Ther* 2012;14:R151.
  21. Sidgwick GP, Iqbal SA, Bayat A. Altered expression of hyaluronan synthase and hyaluronidase mRNA may affect hyaluronic acid distribution in keloid disease compared with normal skin. *Exp Dermatol* 2013;22:377–9.
  22. de la Motte CA, Hascall VC, Drazba J, Bandyopadhyay SK, Strong SA. Mononuclear leukocytes bind to specific hyaluronan structures on colon mucosal smooth muscle cells treated with polyinosinic acid:polycytidylic acid: inter-alpha-trypsin inhibitor is crucial to structure and function. *Am J Pathol* 2003;163:121–33.
  23. Yoshihara Y, Plaas A, Osborn B, Margulis A, Nelson F, Stewart M, et al. Superficial zone chondrocytes in normal and osteoarthritic human articular cartilages synthesize novel truncated forms of inter-alpha-trypsin inhibitor heavy chains which are attached to a chondroitin sulfate proteoglycan other than bikunin. *Osteoarthritis Cartilage* 2008;16:1343–55.
  24. Vignetti D, Karousou E, Viola M, Deleonibus S, De Luca G, Passi A. Hyaluronan: biosynthesis and signaling. *Biochim Biophys Acta* 1840;2014:2452–9.
  25. Fitzpatrick K, Tokish JM. A military perspective to articular cartilage defects. *J Knee Surg* 2011;24:159–66.
  26. Glasson SS, Blanchet TJ, Morris EA. The surgical destabilization of the medial meniscus (DMM) model of osteoarthritis in the 129/SvEv mouse. *Osteoarthritis Cartilage* 2007;15:1061–9.
  27. Fabro AT, da Silva PH, Zocolaro WS, de Almeida MS, Rangel MP, de Oliveira CC, et al. The Th17 pathway in the peripheral lung microenvironment interacts with expression of collagen V in the late state of experimental pulmonary fibrosis. *Immunobiology* 2014;220:124–35.
  28. Chiang MF, Yang SY, Lin IY, Hong JB, Lin SJ, Ying HY, et al. Inducible deletion of the Blimp-1 gene in adult epidermis causes granulocyte-dominated chronic skin inflammation in mice. *Proc Natl Acad Sci USA* 2013;110:6476–81.
  29. Hammaker D, Topolewski K, Edgar M, Yoshizawa T, Fukushima A, Boyle DL, et al. Decreased collagen-induced arthritis severity and adaptive immunity in MKK-6-deficient mice. *Arthritis Rheum* 2012;64:678–87.
  30. Xue H, McCauley RL, Zhang W, Martini DK. Altered interleukin-6 expression in fibroblasts from hypertrophic burn scars. *J Burn Care Rehabil* 2000;21:142–6.
  31. Zhang Q, Yamaza T, Kelly AP, Shi S, Wang S, Brown J, et al. Tumor-like stem cells derived from human keloid are governed by the inflammatory niche driven by IL-17/IL-6 axis. *PLoS One* 2009;4:e7798.
  32. Foley CJ, Kuliopulos A. Mouse matrix metalloproteinase-1a (Mmp1a) gives new insight into MMP function. *J Cell Physiol* 2014;229:1875–80.
  33. Mascaraque C, Aranda C, Ocon B, Monte MJ, Suarez MD, Zarzuelo A, et al. Rutin has intestinal antiinflammatory effects in the CD4+ CD62L+ T cell transfer model of colitis. *Pharmacol Res* 2014;90C:48–57.
  34. Bateman JF, Rowley L, Belluocchio D, Chan B, Bell K, Fosang AJ, et al. Transcriptomics of wild-type mice and mice lacking ADAMTS-5 activity identifies genes involved in osteoarthritis initiation and cartilage destruction. *Arthritis Rheum* 2013;65:1547–60.
  35. Okamoto Y, Hasegawa M, Matsushita T, Hamaguchi Y, Huu DL, Iwakura Y, et al. Potential roles of interleukin-17A in the development of skin fibrosis in mice. *Arthritis Rheum* 2012;64:3726–35.
  36. Mi M, Shi S, Li T, Holz J, Lee YJ, Sheu TJ, et al. TIMP2 deficient mice develop accelerated osteoarthritis via promotion of angiogenesis upon destabilization of the medial meniscus. *Biochem Biophys Res Commun* 2012;423:366–72.
  37. Cook AD, Braine EL, Campbell IK, Hamilton JA. Differing roles for urokinase and tissue-type plasminogen activator in collagen-induced arthritis. *Am J Pathol* 2002;160:917–26.



38. Sun L, Wang X, Kaplan DL. A 3D cartilage - inflammatory cell culture system for the modeling of human osteoarthritis. *Biomaterials* 2011;32:5581–9.
39. Jeong SY, Kim DH, Ha J, Jin HJ, Kwon SJ, Chang JW, et al. Thrombospondin-2 secreted by human umbilical cord blood-derived mesenchymal stem cells promotes chondrogenic differentiation. *Stem Cells* 2013;31:2136–48.
40. Wang Y, Lauer ME, Anand S, Mack JA, Maytin EV. Hyaluronan synthase 2 protects skin fibroblasts against apoptosis induced by environmental stress. *J Biol Chem* 2014;289:32253–65.
41. Matthey DL, Dawes PT, Nixon NB, Slater H. Transforming growth factor beta 1 and interleukin 4 induced alpha smooth muscle actin expression and myofibroblast-like differentiation in human synovial fibroblasts in vitro: modulation by basic fibroblast growth factor. *Ann Rheum Dis* 1997;56:426–31.
42. Pantelidis P, Fanning GC, Wells AU, Welsh KI, Du Bois RM. Analysis of tumor necrosis factor-alpha, lymphotoxin-alpha, tumor necrosis factor receptor II, and interleukin-6 polymorphisms in patients with idiopathic pulmonary fibrosis. *Am J Respir Crit Care Med* 2001;163:1432–6.
43. Krause MP, Moradi J, Nissar AA, Riddell MC, Hawke TJ. Inhibition of plasminogen activator inhibitor-1 restores skeletal muscle regeneration in untreated type 1 diabetic mice. *Diabetes* 2011;60:1964–72.
44. Teunis T, Beekhuizen M, Van Osch GV, Schuurman AH, Creemers LB, van Minnen LP. Soluble mediators in posttraumatic wrist and primary knee osteoarthritis. *Arch Bone Jt Surg* 2014;2:146–50.
45. Ishida Y, Kondo T, Takayasu T, Iwakura Y, Mukaida N. The essential involvement of cross-talk between IFN-gamma and TGF-beta in the skin wound-healing process. *J Immunol* 2004;172:1848–55.
46. Li J, Anemaet W, Diaz MA, Buchanan S, Tortorella M, Malfait AM, et al. Knockout of ADAMTS5 does not eliminate cartilage aggrecanase activity but abrogates joint fibrosis and promotes cartilage aggrecan deposition in murine osteoarthritis models. *J Orthop Res* 2011;29:516–22.
47. Caskey RC, Allukian M, Lind RC, Herdrich BJ, Xu J, Radu A, et al. Lentiviral-mediated over-expression of hyaluronan synthase-1 (HAS-1) decreases the cellular inflammatory response and results in regenerative wound repair. *Cell Tissue Res* 2012;351:117–25.
48. Rilla K, Oikari S, Jokela TA, Hyttinen JM, Karna R, Tammi RH, et al. Hyaluronan synthase 1 (HAS1) requires higher cellular UDP-GlcNAc concentration than HAS2 and HAS3. *J Biol Chem* 2013;288:5973–83.
49. Siiskonen H, Karna R, Hyttinen JM, Tammi RH, Tammi MI, Rilla K. Hyaluronan synthase 1 (HAS1) produces a cytokine- and glucose-inducible, CD44-dependent cell surface coat. *Exp Cell Res* 2014;320:153–63.
50. Olson SA, Horne P, Furman B, Huebner J, Al-Rashid M, Kraus VB, et al. The role of cytokines in posttraumatic arthritis. *J Am Acad Orthop Surg* 2014;22:29–37.